Selective nanomolar detection of dopamine using a boron-doped diamond electrode modified with an electropolymerized sulfobutylether-β- cyclodextrin-doped poly(N-acetyltyramine) and polypyrrole composite film

Shang, Fengjun; Zhou, Lin; Mahmoud, Khaled A.; Hrapovic, Sabahudin; Liu, Yali; Moynihan, Humphrey A.; Glennon, Jeremy D.; Luong, John H. T.

Publisher's version / Version de l'éditeur:
http://dx.doi.org/10.1021/ac900368m
Analytical Chemistry, 81, 10, pp. 4089-4098, 2009-04-21

Anal. Chem. **2009,** *81,* 4089–4098

Selective Nanomolar Detection of Dopamine Using a Boron-Doped Diamond Electrode Modified with an Electropolymerized Sulfobutylether-β-cyclodextrin-Doped Poly(*N*-acetyltyramine) and Polypyrrole Composite Film

Fengjun Shang,[†] Lin Zhou,[†] Khaled A. Mahmoud,[‡] Sabahudin Hrapovic,[‡] Yali Liu,[‡] Humphrey A. Moynihan,[†] Jeremy D. Glennon,[†] and John H. T. Luong*[,†,‡]

Analytical and Biological Chemistry Research Facility (ABCRF), Department of Chemistry, University College Cork, Cork, Ireland, and Biotechnology Research Institute, National Research Council Canada, Montreal, Quebec, Canada H4P2R2

***N*-Acetyltyramine was synthesized and electropolymerized together with a negatively charged sulfobutylether-β-cyclodextrin on a boron-doped diamond (BDD) electrode followed by the electropolymerization of pyrrole to form a stable and permselective film for selective dopamine detection. The selectivity and sensitivity of the formed layer-by-layer film was governed by the sequence of deposition and the applied potential. Raman results showed a decrease in the peak intensity at 1329 cm^{-1} (sp^3), the main feature of BDD, upon each electrodeposition step. Such a decrease was correlated well with the change of the charge-transfer resistance derived from impedance data, i.e., reflecting the formation of the layer-by-layer film. The polycrystalline BDD surface became more even with lower surface roughness as revealed by scanning electron and atomic force microscopy. The modified BDD electrode exhibited rapid response to dopamine within 1.5−2 s and a low detection limit of 4−5 nM with excellent reproducibility. Electroactive interferences caused by 4-dihydroxyphenylalanine, 3,4-dihydroxyphenylacetic acid, ascorbic acid, and uric acid were completely eliminated, whereas the signal response of epinephrine and norepinephrine was significantly suppressed by the permselective film.**

Dopamine (DA) biosynthesized from 4-dihydroxyphenylalanine (L-DOPA) and its two metabolites, epinephrine (EP) and norepinephrine (NEP), are vital neurotransmitters of the central nervous system.[1] DA can be supplied as a medication that acts on the sympathetic nervous system, producing effects such as increased heart rate and blood pressure. However, high catecholamine levels are cardiotoxic, leading to rapid heart rate, high blood pressure, and possible death of the heart muscles.[2] In contrast, a deficiency of DA in the basal ganglia, caused by the degeneration of dopaminergic neurons in the nigrostriatal pathway, is related to Parkinson's disease.[3−5] L-DOPA, the biosynthetic precursor of DA, has been used to alleviate the symptoms of Parkinson's disease and dopa-responsive dystonia because it can cross the blood−brain barrier.[6,7] Therefore, physiological determination of dopamine with high sensitivity and selectivity is of great clinical significance.

Different analytical methods have been reported for DA.[8−11] In brief, fluorometry is sample-consuming and lacks selectivity, whereas chromatography combined mostly with mass spectrometry requires sample pretreatment, lengthy analysis times, and high costs.[3] Electrochemical strategies, advantageous in rapidity and low cost, have been widely employed for the detection of DA. However, early efforts to detect DA using metallic electrodes ran into several severe problems. First, dopamine itself can be electropolymerized, leading to electrode fouling and degradation of response. Second, dopamine is commonly found in conjunction with other materials including its common oxidizable metabolites which interfere drastically with detection, as does the ubiquitous ascorbic acid (AA). The third problem is that physiological concentrations of dopamine are very low, requiring very high selectivity and sensitivity. In the extracellular fluid of the central nervous system, DA ranges from 0.01 to 1 μM[5] compared to 100−500 μM for AA. Both DA and AA also exhibit nearly identical redox potential ranges and comparable sensitivities; thus, it is not possible to detect DA selectively by the known plain electrodes. Electrode fouling problems associated with dopamine polymeri-

* To whom correspondence should be addressed.
[†] University College Cork.
[‡] National Research Council Canada.

(1) Kopin, I. *Pharmacol. Rev.* **1985**, *37*, 333–364.
(2) Wu, H.-P.; Cheng, T.-L.; Tseng, W.-L. *Langmuir* **2007**, *23*, 7880–7885.
(3) Kim, J.; Jeon, M.; Paeng, K.-J.; Paeng, I. R. *Anal. Chim. Acta* **2008**, *619*, 87–93.
(4) Routh, J. I.; Bannow, R. E.; Fincham, R. W.; Stoll, J. L. *Clin. Chem.* **1971**, *17*, 867–871.
(5) Ali, S. R.; Ma, Y.; Parajuli, R. R.; Balogun, Y.; Lai, W. Y.-C.; He, H. *Anal. Chem.* **2007**, *79*, 2583–2587.
(6) Zhan, F.-L.; Kuo, L.-M.; Wang, S.-W.; Lu, M. S.-C.; Chang, W.-Y.; Lin, C.-H.; Yang, Y.-S. *Sens. IEEE* **2007**, *28/31*, 1448–1451.
(7) Hermans, A.; Seipel, A. T.; Miller, C. E.; Wightman, R. M. *Langmuir* **2006**, *22*, 1964–1969.
(8) Zhu, X.; Ge, X. X.; Jiang, C. Q. *J. Fluoresc.* **2007**, *17*, 655–661.
(9) Zhang, L.; Teshima, N.; Hasebe, T.; Kurihara, M.; Kawashima, T. *Talanta* **1999**, *50*, 677–683.
(10) Musshoff, F.; Schmidt, P.; Dettmeyer, R.; Priemer, F.; Jachau, K.; Madea, B. *Forensic Sci. Int.* **2000**, *113*, 359–366.
(11) Patel, B. A.; Arundell, M.; Parker, K. H.; Yeoman, M. S.; O'Hare, D. *J. Chromatogr., B* **2005**, *818*, 269–276.

10.1021/ac900368m CCC: $40.75 © 2009 American Chemical Society
Published on Web 04/21/2009

zation can be circumvented by using modified electrodes that inhibit polymer formation either physically, as, for example, by using self-assembled monolayers, or by a combination of this and modification of potential distribution as occurs in most electropolymerized films, including polypyrrole. The boron-doped diamond (BDD) thin-film electrode, featuring a high current density, wide potential window, low background current, extreme electrochemical stability, and high resistance to fouling, has proven promising for DA detection.[12−14] Electropolymerization, an attractive method for development of bioanalytical devices, allows reproducible, precise, uniform, and thickness-controlled polymer coatings without limitations of the size, area, and geometry of the surfaces.[15−17]

Among the numerous electropolymerizable monomers, pyrrole (Py) is by far the most extensively studied. This biocompatible and water-soluble monomer is easily oxidizable, commercially available, and stable.[18,19] Owing to its intrinsic properties, electrodeposited conductive polypyrrole (PPy) has been employed for the construction of sensors for hydrogen peroxide,[20] glucose,[21] caffeine,[22] phenol,[23] and other target analytes. In comparison to their conducting counterparts, electropolymerized nonconducting polymers are considerably thinner (∼10−100 nm) due to their self-limiting nature.[24] Polytyramine (PTy) is a strongly adhering film,[24] with considerable advantages over other electrodeposited polymers with respect to fast response, reproducibility, and the ability to screen out interferences.[25−28] Recently, electropolymerization of tyramine on a BDD thin-film electrode has demonstrated considerable permselectivity to DA against ascorbic acid, uric acid (UA), L-DOPA, and other DA metabolites.[29] Entrapment of glucose oxidase and sulfobutylether-β-cyclodextrin (SBCD) in the electrodeposited polytyramine has been investigated for highly selective glucose detection with remarkable stability and selectivity.[30]

This paper describes a novel procedure for forming a permselective film on BDD electrodes by subsequent electrodeposition of SBCD-containing *N*-acetyltyramine and pyrrole. The use of *N*-acetyltyramine is advocated to impart surface hydrophobicity to alleviate surface fouling, one of the major drawbacks of conductive hydrophilic surfaces. The incorporation of negatively charged SBCD into the electrodeposited film is anticipated to absorb or even preconcentrate DA while rejecting negative charged UA and AA. The layer-by-layer electropolymerized thin film is characterized by Raman and impedance spectroscopy. The analytical performance of the dopamine sensor with respect to sensitivity and selectivity is presented and discussed in detail. To our knowledge, this is the first modified BDD sensor with considerable selectivity and sensitivity for dopamine.

EXPERIMENTAL SECTION

Chemicals. Tyramine, sodium carbonate, acetic anhydride, Py, DA, L-DOPA, 3,4-dihydroxyphenylacetic acid (DOPAC), EP, NEP, AA, and UA were purchased from Sigma-Aldrich (Dublin, Ireland). SBCD with a degree of substitution (ds) of 4 was obtained from CyDex Pharmaceuticals (Lenexa, KS). Deionized water (18.2 MΩ·cm) was obtained from a Milli-Q (Millipore, Bedford, MA) water purification system. All reagents were of analytical grade with highest purity.

Synthesis of Pyrrole-1-propionic Acid (PPA) and *N*-Acetyltyramine (AcTy). Pyrrole-1-propionic acid was synthesized from pyrrole-1-propionitrile as described by Shang el al.[30] *N*-Acetyltyramine was synthesized according to Valoti et al.[31] with slight variation. In brief, to a solution of tyramine (3 g) in 600 mL of 1 M sodium carbonate, acetic anhydride (2.16 mL) was added slowly. The reaction mixture was stirred at room temperature for 4 h, followed by acidification (pH = 2) by dropwise addition of 5 M HCl. The solution volume was reduced by approximately one-half in vacuo, and the resulting precipitate was isolated by filtration. The filtrate was refluxed in ethyl acetate for 2 h and filtered. The resulting solution was refrigerated overnight, and the formed precipitate was isolated by filtration to yield white crystals (∼1 g, 25% yield). FT-IR (Bruker, Tensor27, Milton, ON, Canada) (KBr, υ_{max}/cm^{-1}): 3335 (m, N−H), 1631 (s, NH−C=O).[32] ^{1}H NMR (Bruker Biospin NMR, Banner Lane, Coventry, U.K.) DMSO-d_6 (δ in ppm): 9.21 (1H, OH), 6.95 (2H, t, ArH), 6.65 (2H, t, ArH), 3.15 (2H, m, CH_2−NH), 2.65 (2H, m, Ph−CH_2), 1.78 (3H, s, CH_3) (see the Supporting Information).

Electrode Preparation. BDD, 3 mm diameter, 0.1% doped boron (Windsor Scientific, Slough, Berkshire, U.K.) was polished with polishing paper (grid 2000, Hand American Made Hardwood Products, South Plainfield, NJ) and subsequently with alumina (Buehler, Markham, ON, Canada) until a mirror finish was obtained. After thorough rinsing with deionized water, the electrode was sonicated in 2-propanol and deionized water for 5 and 10 min, respectively. The electrode was transferred to an electrochemical cell for cleaning by cyclic voltammetry between −0.5 and +2.0 V versus Ag/AgCl (3 M NaCl, BAS, West Layette, IN) at 100 mV s^{-1} in 50 mM phosphate buffer, pH 7 until a stable CV profile was obtained. For field emission scanning electron microscopy (FE-SEM) and atomic force microscopy (AFM) analysis, due to the height limitation of the FE-SEM

(12) Pelskov, Y. V.; Sakharova, A. Y.; Krotova, M. D.; Bouilov, L. L.; Spitsyn, B. V. *J. Electroanal. Chem.* **1987**, *228*, 19–27.
(13) Roy, P. R.; Saha, M. S.; Okajima, T.; Park, S.-G.; Fujishima, A.; Ohsaka, T. *Electroanalysis* **2004**, *16*, 1777–1784.
(14) Wei, M.; Sun, L.-G.; Xie, Z.-Y.; Zhii, J.-F.; Fujishima, A.; Einaga, Y.; Fu, D.-G.; Wang, X.-M.; Gu, Z.-Z. *Adv. Funct. Mater.* **2008**, *18*, 1414–1421.
(15) Cosnier, S. *Anal. Bioanal. Chem.* **2003**, *377*, 507–520.
(16) Chung, T. D.; Jeong, R.-A.; Kang, S. K.; Kim, H. C. *Biosens. Bioelectron.* **2001**, *16*, 1079–1087.
(17) Yuqing, M.; Jianrong, C.; Xiaohua, W. *Trends Biotechnol.* **2004**, *22*, 227–231.
(18) Hu, W.; Li, C. M.; Cui, X.; Dong, H.; Zhou, Q. *Langmuir* **2007**, *23*, 2761–2767.
(19) Sadki, A.; Schottland, P.; Brodiec, N.; Sabouraud, G. *Chem. Soc. Rev.* **2000**, *29*, 283–293.
(20) Li, G.; Wang, Y.; Xu, H. *Sensors* **2007**, *7*, 239–250.
(21) Li, G.; Lin, X. *Biosens. Bioelectron.* **2007**, *22*, 2898–2905.
(22) Ebarvia, B. S.; Cabanilla, S.; Sevilla, F. *Talanta* **2005**, *66*, 145–152.
(23) Korkut, S.; Keskinler, B.; Erhan, E. *Talanta* **2008**, *76*, 1147–1152.
(24) Dubois, J.-E.; Lacaze, P. C.; Pham, M. C. *J. Electroanal. Chem.* **1981**, *117*, 233–241.
(25) Situmorang, M.; Gooding, J. J.; Hibbert, D. B.; Barnett, D. *Biosens. Bioelectron.* **1998**, *13*, 953–962.
(26) Situmorang, M.; Gooding, J. J.; Hibbert, D. B. *Anal. Chim. Acta* **1999**, *394*, 211–223.
(27) Situmorang, M.; Hibbert, D. B.; Gooding, J. J.; Barnett, D. *Analyst* **1999**, *124*, 1775–1779.
(28) Situmorang, M.; Hibbert, D. B.; Gooding, J. J. *Electroanalysis* **2000**, *12*, 111–119.
(29) Shang, F.; Liu, Y.; Hrapovic, S.; Glennon, J. D.; Luong, J. H. T. *Analyst* **2009**, *134*, 519−527 DOI: 10.1039/b814317j.
(30) Shang, F.; Glennon, J. D.; Luong, J. H. T. *J. Phys. Chem. C* **2008**, *112*, 20258–20263.
(31) Valoti, M.; Moron, J. A.; Benocci, A.; Sgaragli, G.; Unzeta, M. *Biochem. Pharmacol.* **1998**, *55*, 37–43.

detection chamber (3 cm maximum), BDD plates (3 mm in diameter, 1200 ppb boron) from Adamant Technologies, La Chaux-de-Fonds, Switzerland were employed instead of the BDD electrode (with the height over 4 cm). The BDD plate was mounted on adhesive copper tape (3 M copper foil tape, Elk Grove Village, IL), and only its active surface was exposed to the electopolymerization using Plasti Dip Performix (Plasti Dip Int., Blaine, MN), a synthetic rubber coating with excellent electrical insulation properties.

Electropolymerization. AcTy (0.1 M) and SBCD (10 mM) were dissolved in 0.3 M NaOH aqueous solution and electropolymerized on the BDD electrode by cycling the potential between −0.1 and +1.7 V versus Ag/AgCl at 500 mV s^{-1} for 40 cycles.[30] The PAcTy/SBCD-modified BDD electrode was rinsed thoroughly with deionized water. Pyrrole was then electrodeposited on the PAcTy/SBCD-modified BDD electrode from 50 mM Py in 50 mM phosphate buffer, pH 7.0 by cycling the potential between −0.1 and +1 V versus Ag/AgCl at 50 mV s^{-1} for 10 cycles. The resulting electrode was denoted as the PPy/PAcTy/SBCD-modified BDD electrode. For comparison, various combinations of polymer film-modified BDD electrodes were also prepared under similar conditions.

Instrumentation. Electropolymerization, cyclic voltammetry (CV) and amperometric (I/t) experiments were performed using CHI 1040A and CHI 601A electrochemical workstations (CH Instruments, Austin, TX). The ac impedance analysis was performed with an EG&G potentiostat (Perkin-Elmer, formally EG/G, Princeton Applied Research, model 6310, Oak Ridge, TN). The impedance measurements were run at a biased potential of E° = 480 mV with 5 mV (rms) sinusoidal excitation amplitude. With $[Fe(CN)_6]^{3-/4-}$ as the redox couple, the impedance data were measured and collected for 21 harmonic frequencies from 0.1 Hz to 100 kHz at five steps/decade and then were analyzed using the ZSimpWin software (Princeton Applied Research). All measurements were performed at room temperature (22−24 °C) using a three-electrode system consisting of a BDD working electrode, a Ag/AgCl (3 M NaCl) reference electrode, and a platinum wire counter electrode.

Scanning electron microscopy micrographs of the bare and modified BDD electrodes were obtained using a Hitachi scanning electron microscope (S-2600 N, Tokyo, Japan), operated in high-vacuum and variable pressure (15 kPa) mode at 4−20 kV with a working distance of 4−20 mm. For higher resolution SEM, a Hitachi FE-SEM S-4800 operated at acceleration voltage of 1.2 kV and a 2.5−6 mm working distance was used. Atomic force microscopy was used to probe the morphology of the bare BDD electrode and the PPy/PAcTy electropolymerized film. AFM micrographs were obtained using a Nanoscope IV (Digital Instruments, Veeco, Santa Barbara, CA) with a silicon tip operated in tapping mode. Raman spectra of the bare BDD, the PAcTy/SBCD-modified BDD, and the PPy/PAcTy/SBCD-modified BDD electrodes were obtained using a custom-made adapter to align the electrode perpendicularly under the laser beam. Raman spectra were acquired by a microconfocal Raman analyzer (LabRAM HR 800, Horiba/Jobin-Yvon, Longjumeau, France) equipped with a frequency-doubled Nd:YAG 532.1 nm laser operating at 200 mW.

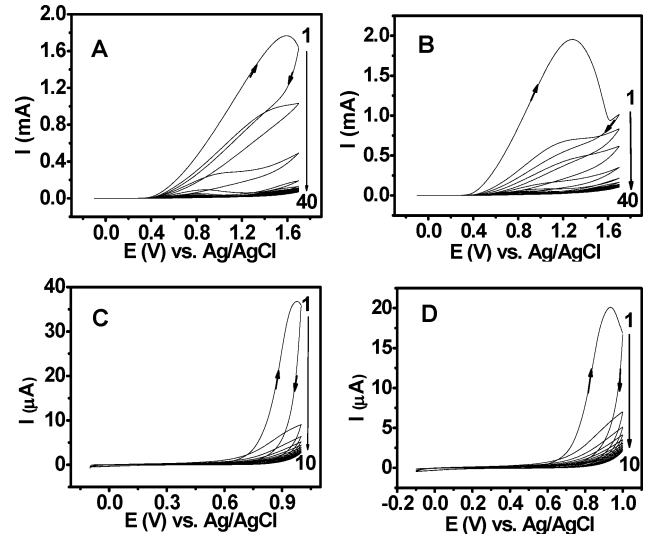

Figure 1. (A) Electropolymerization of 0.1 M *N*-acetyltyramine (AcTy) in 0.3 M NaOH on the BDD electrode. Cyclic voltammetry (CV) was performed from −0.1 to +1.7 V (vs Ag/AgCl) at 0.5 V s^{-1} for 40 cycles. (B) Electropolymerization of 0.1 M *N*-acetyltyramine and 10 mM SBCD in 0.3 M NaOH on the BDD electrode. CV was performed from −0.1 to +1.7 V (vs Ag/AgCl) at 0.5 V s^{-1} for 40 cycles. (C) Electropolymerization of 50 mM pyrrole in 50 mM phosphate buffer, pH 7.0 on the PAcTy-modified BDD electrode. CV was performed from −0.2 to +1.0 V (vs Ag/AgCl) at 0.05 V s^{-1} for 10 cycles. (D) Electropolymerization of 50 mM pyrrole in 50 mM phosphate buffer, pH 7.0 on the PAcTy/SBCD-modified BDD electrode. CV was performed from −0.2 to +1.0 V (vs Ag/AgCl) at 0.05 V s^{-1} for 10 cycles.

RESULTS AND DISCUSSION

Layer-by-Layer Electropolymerization. The choice of the solvent and the electrolyte is of particular importance for electropolymerization since both solvent and electrolyte should be stable at the oxidation potential of the monomer and provide an ionically conductive medium.[19] The film thickness could be adjusted by pH, electrodeposition cycles, scan rate, and the extension of the forced voltage.

First, a layer of AcTy was electropolymerized on BDD as described in the Experimental Section. As estimated by the ACD/Structure Designer software (Advanced Chemistry Development, Toronto, ON, Canada), the aqueous solubility of AcTy (MW 179.22) at pH below 7.4 is only ~14.81 mg/mL compared to 1000 mg/mL for tyramine. However, at pH 10, its solubility is up to 29.78 mg/mL compared with 19.75 for tyramine. Therefore, the electropolymerization of AcTy was performed using 0.1 M AcTy in 0.3 M NaOH. Figure 1A shows the cyclic voltammograms of the potentiodynamic polymerization of AcTy on the BDD electrode. Similar to the electropolymerization of tyramine,[29] the CV profile obtained by AcTy in 0.3 M NaOH revealed a current peak at +1.58 V in the first sweep segment, indicating the oxidation of the phenoxide ion to the free radical intermediate. No reduction throughout the reverse potential sweep was observed, reflecting irreversible electrochemical behavior. From the second to the fourth cycles, the anodic peak current decreased continually, followed by a trend of stabilization in the subsequent cycles. Increasing the number of deposition cycles, reflecting increasing film thicknesses, decreased the signal response of DA, whereas its permselectivity against L-DOPA, DOPAC, AA, and UA was significantly improved. Therefore, 40 cycles was considered as

Scheme 1. Schematic Oxidation and Polymerization of *N*-Acetyltyramine[a]

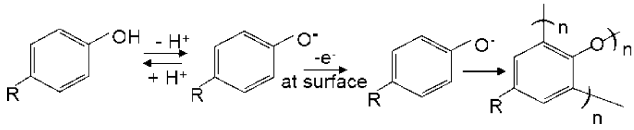

[a] R: $-(CH_2)_2-NH-OCH_3$.

the best compromise. As a phenol derivative, the electrooxidation of AcTy produced phenoxy radicals, which in turn reacted with a neighboring AcTy molecule to form a para-linked dimer. Further oxidation led to oligomers and the eventual formation of an insulating thin film (PAcTy). The acetylated terminal is separated from the phenolic ring by two methylene groups and one imino group; hence, only the phenol moiety is oxidized to perform the polymerization as shown in Scheme 1.[24,25] Polymer layers produced in more alkaline medium usually present self-limiting growth with a thickness of several tens of nanometers due to the layer high resistivity.[25,26,33] In contrast, the film thickness prepared in $HClO_4$ (pH 2) varies from 50 nm to 1.2 μm, depending on the deposition cycles.[34]

When PAcTy was formed on the BDD electrode in the presence of 10 mM SBCD (Figure 1B), the resulting CV profile was similar to that of the electropolymerization without SBCD (Figure 1B). However, there was a negative shift of the peak potential to +1.28 V and more significant current decrease after each cycle, suggesting a faster electron transport across the resulting PAcTy/SBCD film.[35] Phenol has been known to form an inclusion complex with α-cyclodextrin (α-CD) or β-CD with a binding constant of 87 and 214 M^{-1}, respectively, as determined by near-infrared spectroscopy.[36] Similarly, phenol derivatives also display inclusion complexation with β-CD.[37] Therefore, it was reasoned that hydrophobic PAcTy formed an inclusion complex with SBCD to form a host−guest complex and SBCD would be retained on the electrode due to its large chemical dimension.

Finally, in order to further improve the film permselectivity for dopamine, pyrrole had to be electropolymerized on the PAcTy- and PAcTy/SBCD-modified BDD electrodes. The electrochemical method has an influence on the morphology, appearance, and adhesion of PPy. A nonadhesive dendrite-type polymer is formed when a constant current or potential is used, and the film obtained is poorly homogeneous and some electrolyte is present between the electrode surface and the polymer.[38] In contrast, the film obtained from alternated polarization is shiny black and very adhesive with a smooth and homogeneous surface,[38] resulting from the larger number of equivalent nucleation sites and the growth process.[39] Parts C and D of Figure 1 present the cyclic voltammograms of electropolymerization of pyrrole on the PAcTy- and PAcTy/SBCD-modified BDD electrodes, respectively. The peak current of the electrooxidation of pyrrole on the PAcTy film was about twice that of the one observed on the PAcTy/SBCD film in the first cycle, whereas it was approximately coordinative during the following cycles. After 10 cycles, the electrodes were sufficiently coated with PPy. It was reasoned that electrostatic interaction between PPy and SBCD was the main rationale behind the formation of the stable composite film. Our study also confirmed that pyrrole-1-propionic acid could not be electrodeposited on the PAcTy/SBCD-modified BDD electrode.

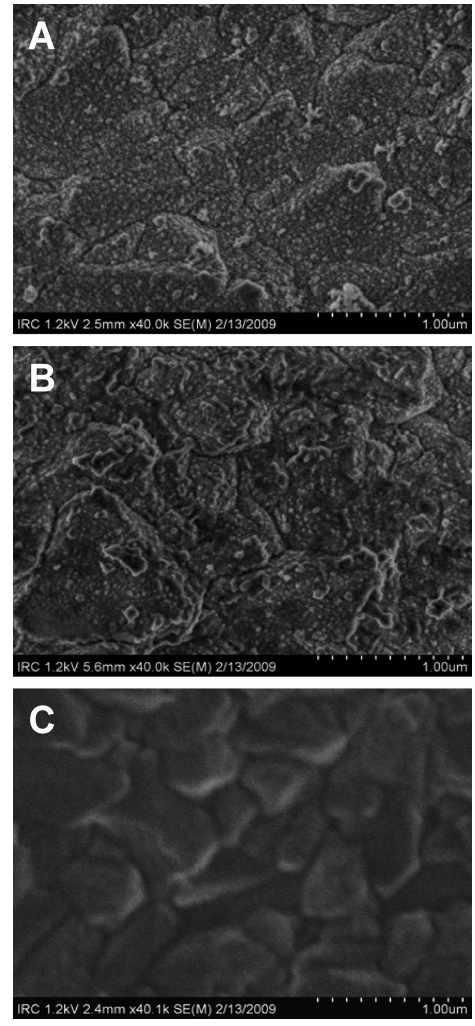

Figure 2. FE-SEM micrographs for the pristine BDD electrode surface before (A) and after the deposition of two layers of PAcTy/SBCD (B) and after the final PPy/PAcTy/SBCD layer (C).

Morphology and Raman Signature of the Modified BDD Electrodes. SEM micrographs acquired by either SEM or FE-SEM could not reveal any significant difference between the surface morphoplogy of the pristine BDD and the PAcTy-modified BDD. Figure 2A shows the polycrystalline feature of the pristine BDD surface. Even after the deposition of two PAcTy layers, the plan-view of SEM images in Figure 2B still exhibited similar feature of pristine BDD, i.e., the surface is composed of many crystallites or grains of varying size, shape, and orientation with

(32) Kemami Wangun, H. V. Isolation, Structure Elucidation and Evaluation of Anti-inflammatory and Anti-infectious Activities of Fungal Metabolites. Ph.D. Dissertation, Friedrich-Schiller-Universität Jena, 2006.
(33) Tenreiro, A. M.; Nabais, C.; Correia, J. P.; Fernandes, F. M. S. S.; Romero, J. R.; Abrantes, L. M. *J. Solid State Electrochem.* **2007**, *11*, 1059–1069.
(34) Tran, L. D.; Piro, B.; Pham, M. C.; Ledoan, T.; Angiari, C.; Dao, L. H.; Teston, F. *Synth. Met.* **2003**, *139*, 251–262.
(35) de Castro, C. M.; Vieira, S. N.; Gonçalves, R. A.; Brito-Madurro, A. G.; Madurro, J. M. *J. Mater. Sci.* **2008**, *43*, 475–482.
(36) Tran, C. D.; De Paoli Lacerda, S. H. *Anal. Chem.* **2002**, *74*, 5337–5341.
(37) Flores, J.; Jimenez, V.; Belmar, J.; Mansilla, H. D.; Alderete, J. B. *J. Inclusion Phenom. Macrocyclic Chem.* **2005**, *53*, 63–68.
(38) Otero, T. F.; DeLaretta, E. *Synth. Met.* **1988**, *26*, 79–88.
(39) Kiani, M. S.; Mitchell, G. R. *Synth. Met.* **1992**, *48*, 203–218.

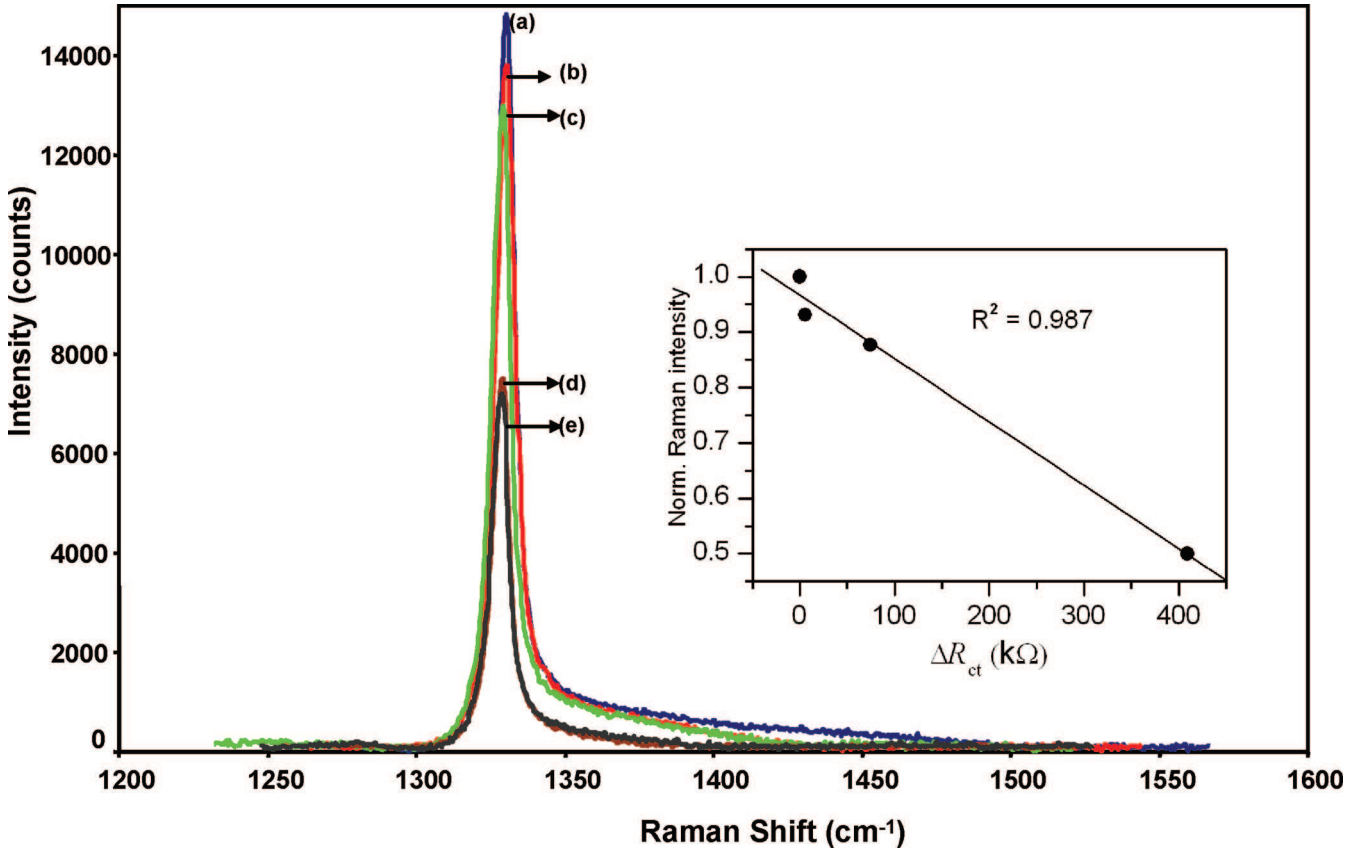

Figure 3. Raman signatures at 1329 cm^{-1} (sp^3) for pristine boron-doped diamond electrode (curve a), after the electropolymerization of the first layer of PAcTy/SBCD (curve b), second layer of PAcTy/SBCD (curve c), and final layer containing PPy plus two PAcTy/SBCD layers (curve d). The overoxidation of PPy on the double PAcTy/SBCD layer is represented by curve e. The inset illustrates the relationship between the normalized peak intensity at 1329 cm^{-1} (sp^3) with the increase in the charge-transfer resistance (R_{ct}) after each step of electropolymerization. The laser was focused on the center of the BDD electrode by an *XYZ* micromanipulator, Raman mapping was carried out to acquire 100 separate Raman spectra, and the area of highest density was chosen for further analysis with the five highest values being averaged.

distinct boundaries. Such crystallites themselves, ranging from 200 to 600 nm, were composed of nanoscale polycrystalline grains. Only after the deposition of the final PPy/PAcTy layer, the surface became smoother and nanoscale diamond crystals were no longer observable (Figure 2C). Owing also to the charging effect, SEM images of the PPy/PAcTy layer on the BDD rendered much less contrast compared to the bare BDD surface or the PAcTy-modified BDD. From AFM analysis, the BDD surface roughness was determined as $R_a = 149.8 \pm 38$ nm, based on 10 measurements over a 100 μm^2 surface (Figure S2A, Supporting Information). The BDD surface was uneven as reflected by a very large standard deviation; thus, AFM imaging did not reveal any significant difference between the pristine BDD from the modified counterpart. Nevertheless, for the PPy/PAcTy-modified BDD surface, the mean roughness was noticeably smaller ($R_a = 124.4 \pm 13$ nm). Apparently, the electropolymerized film was mostly deposited on the edges of the polycrystallites and the valley region, resulting in a more even and smoother surface (Figure S2B, Supporting Information).

Raman spectroscopy was conducted to characterize the electropolymerized film on the BDD electrode since the Raman signature of the pristine BDD electrode should exhibit one intense band at 1329 cm^{-1} (sp^3), the first-order phonon mode for diamond. As expected, the Raman spectrum for the pristine BDD electrode featured one intense band at 1329 cm^{-1} (sp^3) with no indication of graphitic impurities as shown in Figure 3, curve a, in agreement with Shang et al.[30] The electrodeposition of the first layer of the PAcTy/SBCD film on the BDD electrode significantly reduced the peak intensity from 14 722 to 13 703 or 1019 counts (Figure 3, curve b). The second layer of the PAcTy/SBCD film was somewhat thinner as reflected by a smaller decrease of the peak intensity from 13 703 to 12 905 or 798 counts (Figure 3, curve c). In accordance with Shang et al.,[30] such a decrease in the Raman intensity should correspond to formation of an electropolymerized film with a thickness of ~22 nm. The formation of PPy on the two-layered PAcTy/SBCD-modified BDD electrode resulted in a significant decrease in the peak intensity from 12 905 to 7416 counts (~5490 counts), due to the additional formation of the thicker PPy layer (Figure 3, curve d), which was estimated to be ~66 nm.[30] Therefore, the combined electropolymerized layer (the PPy layer plus the two PAcTy layers) should have an overall thickness of 85 nm. When PPy was overoxidized (+1.5 V) on the PAcTy/SBCD-modified electrode, the peak intensity was down to 7104, indicating the formation of an even thicker layer (Figure 3, curve e). This phonon mode was much less intense due to the presence of the composite film because the optical density is significantly higher, i.e., the penetration depth of the laser light was smaller. In all cases, the full width at half-maximum (fwhm) and the peak position were slightly affected. Good-quality chemical vapor deposition diamond films should produce peaks with an fwhm of 4−10 cm^{-1}.[30]

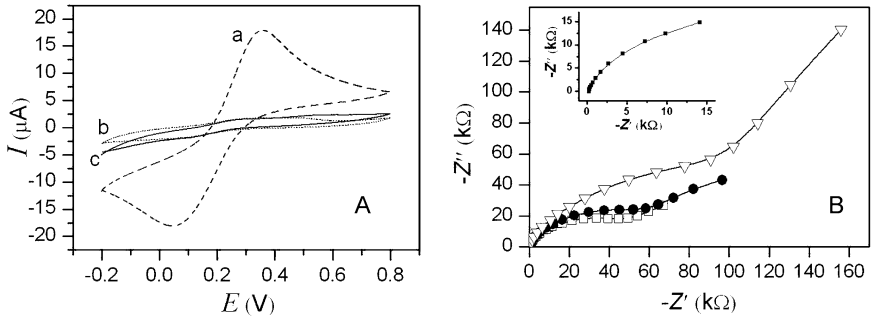

Figure 4. (A) Cyclic voltammograms of (a) bare BDD electrode, (b) two PAcTy/SBCD layers, and (c) two PAcTy/SBCD layers plus the PPy layer. CVs were measured at 0.1 V s^{-1} in 0.1 M KNO_3 containing $Fe(CN)_6^{3-/4-}$ as the redox probe. A 3 M Ag/AgCl and a platinum wire were used as reference and counter electrodes, respectively. (B) The Nyquist plots for the Faradic impedance in 0.1 M KNO_3 containing 5 mM $Fe(CN)_6^{3-/4-}$ as the redox probe for BDD blank (■), shown as the inset, one PAcTy/SBCD layer (□), two PAcTy/SBCD layers (●), and PPy plus two PAcTy/SBCD layers (▽). The impedance spectra were recorded from 0.1 Hz to 100 kHz at the formal potential of the redox couple. The amplitude of the alternate voltage was 5 mV. The symbols represent the experimental data, and the solid lines are the fitted curves using the equivalent circuit. A 3 M Ag/AgCl and platinum wire were used as reference and counter electrodes, respectively.

Scheme 2. Equivalent Circuit Model for Mixed Kinetic and Diffusion Control[a]

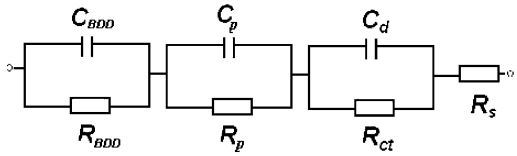

[a] R_s, solution resistance; C_d, double layer capacitance; R_{ct}, charge-transfer resistance; $(CR)_p$ and $(CR)_{BDD}$, capacitor and resistor due to the polymer layers and the BDD electrode, respectively.

Characteristics of the Modified BDD Electrodes. The layer-by-layer electropolymerization of AcTy and Py on the BDD electrode was evaluated by CV in presence of 0.1 M KNO_3 with 5 mM $Fe(CN)_6^{3-/4-}$ as the redox probe. The CVs show an obvious blockage on the electrode surface due to the polymerized films of AcTyr and Py, respectively (Figure 4A). The ac impedance spectra were acquired to elucidate the electrode/solution interface during the electrodeposition process. Figure 4B shows the Nyquist plot (real Z' versus imaginary Z'') of the BDD electrode after being modified with the first and second PAcTy layers, respectively, followed by the formation of the PPy film. The plot exhibited a semicircle near the origin at high frequencies followed by a linear tail with a slope of unity. The ac impedance data were fitted to the equivalent circuit model (Scheme 2) consisting of three Randles circuits in series to represent C_{BDD} for the bare BDD electrode, $(CR)_p$ for the polymer layers, (C_d, R_{ct}) for the electrode/solution interface, and R_s is the solution resistance, except for the bare BDD electrode, where only two Randles circuits in series (CR_{BDD}, C_d, and R_{ct}) were modeled.

The circuit model was used mainly to determine C_d and R_{ct}. Any change in C_d should be negligible compared to the change in R_{ct}. When the $Fe(CN)_6^{3-/4-}$ redox-active couple was blocked by the PAcTy and/or PPy film, the electrodeposition and subsequent interaction events at the electrode were detected by following the change in R_{ct} because of its drastic change compared to C_d or other parameters. Indeed, R_{ct} is the most direct and sensitive parameter that responds to changes on the electrode interface, as represented by the diameter of the semicircle in the Nyquist plot.[40] In brief, the blank BDD electrode exhibited a high charge-transfer resistance (R_{ct} = 1657 Ω), an inherent feature of BDD, compared to other bare electrodes such as gold, platinum, etc. A considerable increase in R_{ct} was observed due to the thickness increase at the PPy/PAcTy/SBCD-modified electrode compared to the bare BDD electrode (Table 1). Such behavior indicated that the electron transfer to the electrode was significantly reduced due to the presence of the electropolymerized PPy/AcTy film. As expected, changes in R_s, C_d, R_{BDD}, and C_{BDD} were insignificant compared to the change in R_{ct}. Nevertheless, it was still possible to observe changes in R_{BDD}, resulting from the electropolymerized film after each electrodeposition step. For instance, an initial increase in R_{BDD} reflected the formation of the nonconducting PAcTy film. However, the electrodeposition of conducting Py resulted in a drastic decrease in R_{BDD} with a resulting value even smaller than that of bare BDD (Table 1). Notice that the data obtained by Raman spectroscopy were corroborated well with those of impedance spectroscopy. As shown in the inset of Figure 3, the decrease in the Raman intensity peak was inversely proportional to ΔR_{ct}.

The ac impedance data were also in a good agreement with the amperometric I/t measurement of the three electrodes (bare BDD electrode, PAcTy/SBCD-modified BDD, and PPy/AcTy/SBCD-modified BDD) in 100 mM phosphate buffer, pH 7. The resulting current measured after 60 s of constantly applied potential (+500 mV vs Ag/AgCl) exhibited the highest value for the bare BDD electrode (18.3 μA). Under the same conditions, this value dropped to 4.1 μA upon the two consecutive AcTy/SBCD polymerizations. Finally, the electropolymerization of the conductive PPy film on top of the double-layered PAcTy/SBCD film contributed in the increase of the resulting current to 9.3 μA (Figure S3, Supporting Information).

Permselectivity of the Modified BDD Electrodes. The relative permselectivity of various BDD electrodes was presented in Table 2, calculated as the response signal ratio for each species relative to DA. The pristine BDD electrode exhibited comparable response signals to DA, L-DOPA, DOPAC, EP, and NEP at the same concentration (20 μM) when poised at +0.8 V. Both AA

(40) Patolsky, F.; Zayats, M.; Katz, B.; Willner, I. *Anal. Chem.* **1999**, *71*, 3171–3180.

Table 1. Simulated Impedance Values of the Bare BDD Electrode before and after Electrodeposition of AcTyr and Py Films, Respectively, as Determined by ac Impedance Spectroscopy

	R_s (Ω)	R_{ct} (Ω)	C_d (F·cm^{-2})	R_p (Ω)	C_p (F·cm^{-2})	R_{BDD} (Ω)	C_{BDD} (F·cm^{-2})
BDD blank	255	1657	6.1×10^{-7}	na	na	27981	5.0×10^{-7}
one PAcTy/SBCD layer	169	7302	6.2×10^{-7}	43 790	7.8×10^{-7}	46 400	2.5×10^{-7}
two PAcTy/SBCD layers	276	76 482	2.2×10^{-5}	56 063	1.7×10^{-6}	56 270	6.7×10^{-7}
PPy/two PAcTy/SBCD layers	228	411 102	1.0×10^{-5}	99 100	1.3×10^{-6}	12 084	4.6×10^{-7}

Table 2. Permselectivity (%) of the Modified BDD Electrodes[a]

analyte	bare (%)	PAcTy (%)	PAcTy/SBCD (%)	PPy/PAcTy (%)	PPy/PAcTy/SBCD (%)
20 μM DA	100	100	100	100	100
0.1 mM AA	1020	292	357	3	0
0.1 mM UA	1050	52	84	0	0
20 μM L-DOPA	80	47	64	0	0
20 μM DOPAC	125	5	4	0	0
20 μM EP	160	127	133	36	29
20 μM NEP	112	91	113	52	39

[a] Calculated by the response signal ratio between each species relative to dopamine.

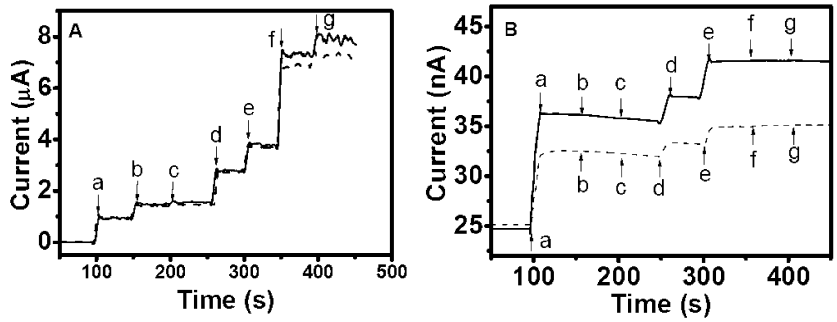

Figure 5. (A) Amperometric response at +0.8 V of the PAcTy-modified BDD (dashed line) and PAcTy/SBCD-modified BDD (solid line) electrodes to the addition of (a) 20 μM DA, (b) 20 μM L-DOPA, (c) 20 μM DOPAC, (d) 20 μM EP, (e) 20 μM NEP, (f) 0.1 mM AA, and (g) 0.1 mM UA in 50 mM phosphate buffer, pH 7.0. (B) Amperometric response at +0.8 V of the PPy/PAcTy-modified BDD (dashed line) and PPy/PAcTy/SBCD-modified BDD (solid line) electrodes to the addition of (a) 20 μM DA, (b) 20 μM L-DOPA, (c) 20 μM DOPAC, (d) 20 μM EP, (e) 20 μM NEP, (f) 0.1 mM AA, and (g) 0.1 mM UA in 50 mM phosphate buffer, pH 7.0.

and UA at their physiological levels (0.1 mM) provoked phenomenal interference, 10-fold higher than that of DA. Such results confirmed the drawback of electrochemical detection of DA using unmodified electrodes. Electropolymerization of AcTy played a dual role in improving selectivity and retaining SBCD. Figure 5A compared the signal response of the PAcTy-modified and PAcTy/SBCD-modified BDD electrodes toward consecutive addition of 20 μM DA, 20 μM L-DOPA, 20 μM DOPAC, 20 μM EP, 20 μM NEP, 0.1 mM AA, and 0.1 mM UA in 50 mM, pH 7 phosphate buffer at 0.8 V. Both electrodes exhibited considerable suppression on DOPAC (~10-fold) and UA (~20-fold). However, AA and L-DOPA still provoked 3-fold and ~70% of the signal response compared to that of DA, respectively, which is different from 15% and 10% obtained from the PTy-modified electrode.[29] This could be attributed to the more porous morphology of the PAcTy and PAcTy/SBCD films. Alleviation of the interferences caused by EP and NEP was more modest compared to others.

Remarkable permselectivity was observed after pyrrole electrodeposition (Figure 5B). Higher response of DA was also observed on the PAcTy/SBCD-modified electrode compared to that in the absence of SBCD, indicating the favorable transport of DA due to the enlarged porosity caused by SBCD entrapment. The signal responses of L-DOPA, DOPAC, AA, and UA were eliminated on the PPy/PAcTy/SBCD-modified electrodes. Notice that even 1 mM AA did not invoke any noticeable response. Apparently, the molecular sieving effect played a crucial role to facilitate their penetration. DA with the minimal chemical structure produced the highest response followed by NEP and EP. A noticeable higher signal response for NEP over EP was somewhat anticipated because NEP and DA are primary amines, whereas EP is a secondary amine. L-DOPA, DOPAC, an in vivo metabolite of dopamine, AA, and UA were rejected due to their bulkier structures. Permselectivity of DA over EP and NEP as well as the total elimination of UA might lead to another important application: measurement of urinary catecholamines, an initial screening test for pheochromocytoma.[41] Notice that the level of EP and NEP is significantly lower than that of DA in urine.[42] The urinary excretion rate (>15 years) of DA, NEP, and EP is 65−400, 1−80, and 0.5−20 μg/day.

A series of experiments was also conducted to reevaluate the permselectivity of the modified BDD electrode at low analyte concentrations. As expected, UA, AA, L-DOPA, and DOPAC (100

(41) Gitlow, S. E.; Mendlowitz, M.; Bertrani, I. M. *Am. J. Cardiol.* **1970**, *26*, 270–279.
(42) Tietz, N. W. *Fundamentals of Clinical Chemistry*, 3rd ed.; W. B. Saunders, Philadelphia, 1987.

nM each) did not provoke any detectable response. The averaged signal for four repeated measurements of EP and NEP (100 nM each) was about 28% and 36.8%, respectively, of the dopamine signal at the same concentration. Such results were in agreement with the data obtained for the three neurotranmitters at 20 μM as discussed earlier. Our experimental data with the bare BDD electrode also confirmed that aspirin, up to 1 mM, was not electroactive as anticipated, whereas the response of acetaminophen was about 55% of the DA signal at the same concentration (5 μM). However, the signal response of acetaminophen exhibited by the PPy/PAcTy/SBCD-modified BDD was only 10% compared to dopamine at the same concentration. Note that ~90% of acetaminophen is normally metabolized by the liver to nontoxic sulfate or glucuronide metabolites and only <9% of acetaminophen is excreted unchanged in the urine. Nevertheless, the replacement of acetaminophen by aspirin could be the best strategy to circumvent any plausible interference of this electroactive compound.

Mechanism Behind the Permselectivity. A series of attempts was conducted to decipher the mechanism behind the preeminent permselectivity. It is of importance to notice that in order to attain the selectivity for DA detection, the PAcTy/SBCD had to be deposited first on the BDD electrode followed by PPy. Experimental data confirmed that electropolymerization in a reverse order (PPy first followed by PAcTy/SBCD) could not sufficiently suppress the interference. Although the PPy-modified BDD electrode demonstrated satisfactory permselectivity against L-DOPA and DOPAC, interference caused by AA and UA was not completely suppressed. Doping of SBCD in the PPy film even adversely affected the selectivity, similar to the results obtained with the PPy/β-CD-modified glassy carbon electrode (GCE),[43] CV profiles of L-DOPA showing no peak at the PPy-modified electrode while displaying a well-defined oxidation peak at the PPy/β-CD-modified electrode. Overoxidized polypyrrole (PPy_{ox}) has been widely investigated for selective detection of dopamine and other catecholamines.[44−48] Such films provide some selectivity for dopamine, but both AA and UA even at 20 μM still provoke detectable response.[48] Our experimental data confirmed that the PPy_{ox}/PAcTy/SBCD-modified BDD electrode exhibited no response to both DA and others, reflecting relatively denser morphology and higher thickness of the PPy_{ox} film compared to PPy as discussed previously (Figure 3). For comparison, a more porous film, poly(pyrrole-1-propionic acid) (PPA), was electrogenerated on the PAcTy/SBCD-modified BDD electrode. Notice that unlike PPy, the PPA-modified BDD electrode displayed the well-defined feature of the ferri-/ferrocyanide redox couple. Experimental data also indicated the inferiority of the PPA/PAcTy/SBCD film toward the rejection of AA and UA. Selective measurement of DA in the presence of AA can also be realized using a Nafion-coated GCE modified with catechin hydrate as a nature antioxidant.[49] However, our experimental data confirmed that the Nafion-coated BDD electrode demonstrated no selectivity toward DA as it responded to all of the analytes. Moreover, the Nafion layer can only be formed by dropping or spreading on the electrode surface, and it is difficult to precisely control the film thickness, uniformity, location, and reproducibility. All of these experiments implied the crucial role of the film morphology with respect to the selectivity and sensitivity.

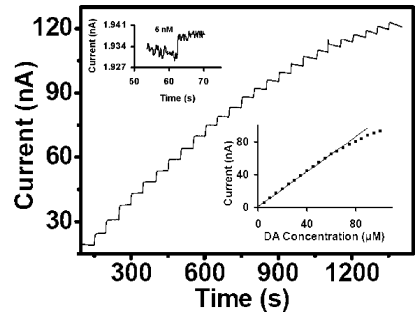

Figure 6. Typical current−time response at +0.8 V of the PPy/PAcTy/SBCD-modified BDD electrode upon successive addition of 5 μM DA in 50 mM phosphate buffer, pH 7.0. The calibration curve was replotted from the data obtained in Figure 4A.

Analytical Performance of the DA Sensor. A typical current−time plot and the calibration curve of the PPy/PAcTy/SBCD-modified BDD electrode at +0.8 V with the successive addition of 5 μM DA are illustrated in Figure 6. The response time was 1.5−2 s with linearity up to 60 μM DA, way beyond the upper level of physiological dopamine (0.01−1 μM). As shown in Figure 6 (upper inset), the detection limit was as low as 5 nM (S/N = 3), compared to 50 nM obtained by the electrode without SBCD. Such a feature could be attributed to the favorable DA penetration with SBCD entrapment and a very low and stable background exhibited by the modified BDD electrode. The combined PPy/PAcTy/SBCD film was very stable due to its strong adhesion to the BDD electrode surface. The sensor was used for at least 25 repeated analyses of 5 μM DA without noticeable surface fouling. If required, the modified electrode could be simply regenerated by electrochemical cleaning from −0.2 V to +0.8 V at 100 mV s^{-1} for a few cycles. In most cases, CV or more sensitive differential pulse voltammetry (DPV) can be used for the selective measurement of dopamine. However, these two common methods do not permit continuous measurement but sample with a frequency depending on the speed of the scan and the length of the regeneration period, which is less attractive for in situ monitoring. Of interest is the modification of a gold electrode with a 11-mercaptoundecanoic acid−poly(ethylene glycol) (MUA−PEG) composite film for sensitive and selective detection of DA in the presence of AA.[50] The modified electrode shows good reproducibility (±2%) and a low detection limit (10 nM). Simultaneous determination of DA, serotonin (5-hydroxytryptamine, or 5-HT), and AA can also be achieved using a nano-Au/PPy_{ox}-modified GCE with a detection limit of 15 nM DA.[51] However, such systems have not been challenged by other electroactive neurotransmitters.

(43) Izaoumen, N.; Bouchta, D.; Zejli, H.; Kaoutit, M. E.; Stalcup, A. M.; Temsamani, K. R. *Talanta* **2005**, *66*, 111–117.
(44) Kang, T.-F.; Shen, G.-L.; Yu, R.-Q. *Talanta* **1996**, *43*, 2007–2013.
(45) Witkowske, A.; Brajter-Toth, A. *Anal. Chem.* **1992**, *64*, 635–641.
(46) Li, Y.; Wang, P.; Wang, L.; Lin, X. *Biosens.Bioelectron.* **2007**, *22*, 3120–3125.
(47) Jiang, X.; Lin, X. *Analyst* **2005**, *130*, 391–396.
(48) Olivia, H.; Shin, S. D.; Rao, T. N.; Fujishima, A. *Analyst* **2002**, *127*, 1572–1575.
(49) Salimi, A.; Abdi, K.; Khayatian, G.-R. *Microchim. Acta* **2004**, *144*, 161–169.
(50) Xiao, Y.; Guo, C.; Li, C. M.; Li, Y.; Zhang, J.; Xue, R.; Zhang, S. *Anal. Biochem.* **2007**, *371*, 229–237.
(51) Li, J.; Lin, X. *Sens. Actuators, B* **2007**, *124*, 486–493.

Although the BDD-modified electrode can detect dopamine as low as 4−5 nM, it is still a formidable task for the reliable detection of dopamine and its metabolites in normal plasma or cerebrospinal fluid. The exact level of plasma dopamine is unknown and somewhat controversial.[52−55] The sample handling or preparation might result to varying degrees in deconjugation of dopamine, as most dopamine in plasma exists in conjugated forms.[56] Variability from study to study could also be derived simply from the use of relatively few subjects with large interindividual differences in resting free dopamine concentrations. The dopamine concentration in some samples could be up to 4.15 nM (635 pg/mL)[56] with the average concentration ranging from 0.4 to 1 nM. The plasma concentration of the two other DA metabolites is also very low: 0.5 nM for EP and 1.6 nM for NEP.[57] The concentration of such three catecholamines is even lower in the cerebrospinal fluid: 0.06 nM for DA, 0.06−1.1 nM for NEP, and 0.05−0.5 nM for EP.[58]

Fast scan cyclic voltammetry (FSCV), when the applied potential is cycled at scan rates >100 V s^{-1}, has proven to be very important in this regard due to the high sensitivity and selectivity.[59,60] At higher scan rates, compounds with slower electron transfer rates like ascorbic acid can be distinguished very easily from organic amines.[61,62] FSCV using carbon fibers is still limited to observing concentration changes over the time course of a minute due to the large background current, which greatly exceeds the faradic current from the redox reaction of solution analytes. Moreover, it is not possible to measure the basal concentration of electroactive species because of the differential nature of the technique.[63,64] BDD electrodes possess very low capacitance and the largest potential window measured in aqueous electrolytes compared with other know electrode materials including carbon-based electrodes. In comparison to BDD, carbon-based electrodes such as graphite and glassy carbon are more vulnerable to surface oxidation and fouling. Notice also that a single liquid chromatography with electrochemical detection assay takes about 1 h, compared with 2 days for the catechol-*O*-methyltransferase radioenzymatic (COMT-RE) technique.[56] Therefore, the modified BDD electrode might still be the method of choice when clinical results are needed quickly, particularly for patients suspected with elevated levels of dopamine. One of important applications is the detection of elevated dopamine in plasma, urine, and tissues of patients with catecholamine-producing paragangliomass.[65] In such patients, the plasma dopamine can be up to ∼360 nM compared to ∼1 nM for EP and ∼88 nM for NEP due to deficiency in tumor cells of dopamine-β-hydroxylase,[66] the enzyme that coverts DA to NEP. Another important feature of the modified BDD electrode was its total insensitivity to L-DOPA, the precursor of dopamine, which could be up to 244 nM in the plasma of such patients.[67] Therefore, the selective detection of dopamine would be anticipated by using the modified BDD electrode, and work is in progress toward this objective.

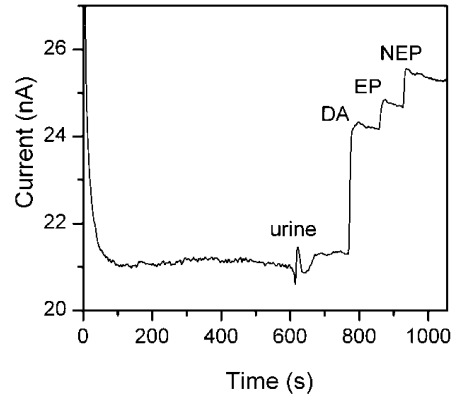

Figure 7. *I*/*t* response of the PPy/PAcTy/SBCD-modified BDD at +0.8 V for 100 nM DA, EP, and NEP spiked in a urine sample. The measurement was performed in 50 mM phosphate buffer, pH 7.0.

Experiments were conducted to evaluate the applicability of the PPy/PacTy/SBCD-modified electrode for analysis of DA, EP, and NEP spiked in a urine sample obtained from a healthy subject. The urine sample alone only provoked a response signal of 0.5 nA (100 μL in a 10 mL detection cell), and the PPy/PAcTy/SBCD-modified BDD electrode exhibited a reproducible response to the urine sample spiked with DA, EP, and NEP, respectively, at 100 nM (Figure 7). Such responses were comparable with those of the modified BDD electrode to the above neurotransmitters prepared in the standard buffer. In contrast, unmodified BDD displayed a very high response to the urine sample with a resulting current increase from 2.56 nA to 1 μA. Such behavior was anticipated due to the presence of uric acid in the urine sample. Spiked neurotransmitters in the urine sample were not detectable unless they were above 10 μM (figure not shown).

CONCLUSIONS

In brief, the modification of the BDD electrode with an electropolymerized PPy/PAcTy/SBCD composite film has led to the fabrication of a highly stable sensor for dopamine with excellent sensitivity and selectivity. Dopamine as low as 4−5 nM was detected, while the interferences caused by AA and UA at their physiological levels were entirely obviated. Even excess concentration of AA (1 mM) did not exhibit salient signal response compared to 20 μM DA. Furthermore, L-DOPA and DOPAC were eliminated and EP and NEP were significantly suppressed by the

(52) Wenk, G.; Greenland, R. *J. Chromatogr.* **1980**, *183*, 261–267.
(53) Moyer, T. P.; Jiang, N. S.; Tyce, G. M.; Sheps, S. C. *Clin. Chem.* **1979**, *25*, 256–263.
(54) DaPrada, M.; Zurcher, G. *Life Sci.* **1976**, *19*, I 161I 174.
(55) Robertson, D.; Johnson, G. A.; Robertson, R. M.; Nies, A. S.; Shand, D. C.; Oates, J. A. *Circulation* **1979**, *59*, 637–643.
(56) Goldstein, D. S.; Feuerstein, G. Z.; Kopin, I. J.; Keiser, H. R. *Clin. Chim. Acta* **1981**, *117*, 113–120.
(57) Goldstein, D. S.; Stull, R.; Zimlichman, R.; Levinson, P. D.; Smith, H.; Keiser, H. R. *Clin. Chem.* **1984**, *30*, 815–816.
(58) Christensen, N. J.; Vestergaard, P.; Sorensen, T.; Rafaelsen, O. J. *Acta Psychiatr. Scand.* **1980**, *61*, 178–182.
(59) Millar, J.; Stamford, J. A.; Kruk, Z. L.; Wightman, R. M. *Eur. J. Pharmacol.* **1985**, *109*, 341–348.
(60) Cahill, P. S.; Walker, Q. D.; Finnegan, J. M.; Mickelson, G. E.; Travis, E. R.; Wightman, R. M. *Anal. Chem.* **1996**, *68*, 3180–3186.
(61) Marsden, C. A.; Joseph, M. H.; Kruk, Z. L.; Maidment, N. T.; Oneill, R. D.; Schenk, J. O.; Stamford, J. A. *Neuroscience* **1988**, *25*, 389–400.
(62) Millar, J.; O'Connor, J. J.; Trout, S. J.; Kruk, Z. L. *J. Neurosci. Methods* **1992**, *43*, 109–118.
(63) Robinson, D. L.; Hermans, A.; Seipel, A. T.; Wightman, R. M. *Chem. Rev.* **2008**, *108*, 2554–2584.
(64) Hermans, A.; Keithley, R. B.; Kita, J. M.; Sombers, L. S.; Wightman, R. M. *Anal. Chem.* **2008**, *80*, 4040–4080.
(65) Eisenhofer, G.; Goldstein, D. S.; Sullivan, P.; Csako, G.; Brouwers, F. M.; Lai, E. W.; Adams, K. T.; Pacak, K. *J. Clin. Endocrinol. Metab.* **2005**, *90* (4), 2068–2075.
(66) Feldman, J. M.; Blalock, J. A.; Zern, R. T.; Shelburne, J. D.; Gaede, J. T.; Farrell, R. E.; Wells, S. A., Jr. *Am. J. Clin. Pathol.* **1979**, *72*, 175–1855.
(67) Eldrup, E. *Dan. Med. Bull.* **2004**, *51* (1), 34–62.

modified BDD electrode. Ultimately, this proof of concept can unravel the selectivity limitations of the in vivo voltammetric detection of neurotransmitters. A miniaturized modified BDD electrode is anticipated to fulfill the requirement for in vivo detection of dopamine. Owing to their chemical inertness and mechanical durability, the application of BDD electrodes for in vivo detection in mouse brains has been attempted.[68] Our precedent procedure is favorable for microelectrode and microarray fabrication toward in vitro monitoring of neurotransmitters, because of a controlled electrodeposition of the permselective films. This can be adopted in the future for in vivo electrochemical searching methods for neurotransmitters by reducing the diameter of the electrode to submicrometer in order to improve the requisite selectivity with minimal tissue damage. This approach also opens up new opportunities for the immobilization of biomolecules toward biosensing and immunoassays.

(68) Suzuki, A.; Ivandini, T. A.; Yoshimi, K.; Fujishima, A.; Oyama, G.; Nakazato, T.; Hattori, N.; Kitazawa, S.; Einaga, Y. *Anal. Chem.* **2007**, *79*, 8608–8615.

ACKNOWLEDGMENT

This work was supported by the Irish Research Council for Science, Engineering and Technology (IRCSET), Ireland, under the Embark Initiative Postgraduate Research Scholarship Scheme (F.S.) and the Science Foundation of Ireland (SFI), the Walton Visitor Award (J.H.T.L.).

SUPPORTING INFORMATION AVAILABLE

IR spectra of tyramine and *N*-acetyltyramine (Figure S1), AFM micrographs of a BDD surface and modified BDD (Figure S2), and the I/t curves for the modified BDD electrode (Figure S3). This material is available free of charge via the Internet at http://pubs.acs.org.

Received for review February 17, 2009. Accepted April 4, 2009.

AC900368M